



Article

Exploring Enhanced Oxygen Reduction Reactions: A Study on Nanocellulose, Dopamine, and Cobalt Complex-Derived Non-Precious Electrocatalyst

Md Mohsin Patwary ¹, Shanzida Haque ^{1,2}, Peter Szwedo ¹, Ghada Hasan ¹, Raja Shekhar Kondrapolu ¹, Fumiya Watanabe ³, Krishna KC ¹, Daoyuan Wang ⁴ and Anindya Ghosh ^{1,*}

- School of Physical Sciences, University of Arkansas at Little Rock, 2801 South University Avenue, Little Rock, AR 72204, USA; mpatwary@ualr.edu (M.M.P.); shaque1@ualr.edu (S.H.); pkszwedo@ualr.edu (P.S.); gfhasan@ualr.edu (G.H.); rkondrapolu@ualr.edu (R.S.K.); kkc@ualr.edu (K.K.)
- Department of Physics, Comilla University, Cumilla 3506, Bangladesh
- Center for Integrative Nanotechnology Sciences, University of Arkansas at Little Rock, 2801 South University Avenue, Little Rock, AR 72204, USA; fxwatanabe@ualr.edu
- Department of Chemistry and Physics, University of Arkansas at Pine Bluff, 1200 North University Drive, Pine Bluff, AR 71601, USA; wangd@uapb.edu
- * Correspondence: axghosh@ualr.edu; Tel.: +1-501-916-5197; Fax: +1-501-569-8838

Abstract: Cobalt-based catalysts are recognized as promising electrocatalysts for oxygen reduction reactions (ORRs) in fuel cells that operate within acidic electrolytes. A synthesis process involving a cobalt complex, nanocellulose, and dopamine, followed by pyrolysis at 500 °C under a nitrogen atmosphere, was used to create a cobalt and nitrogen-doped carbonaceous material. Additionally, urea was incorporated to enhance nitrogen doping in the carbonaceous material. The morphology and structure of the material were examined using Scanning Electron Microscopy (SEM) and X-ray Diffraction (XRD), where SEM unveiled dispersed metal oxides within the carbonaceous framework. Energy Dispersive X-ray Spectroscopy (EDS) analysis showed an even distribution of elements across the cobalt-doped carbonaceous material. X-ray Photoelectron Spectroscopy (XPS) analysis further highlighted significant alterations in the elemental composition due to pyrolysis. The electrochemical behavior of the cobalt-doped carbonaceous material, with respect to the oxygen reduction reaction (ORR) in an acidic medium, was investigated via cyclic voltammetry (CV), revealing an ORR peak at 0.30 V against a reversible hydrogen reference electrode, accompanied by a notably high current density. The catalyst's performance was evaluated across different pH levels and with various layers deposited, showing enhanced effectiveness in acidic conditions and a more pronounced reduction peak with uniformly applied electrode layers. Rotating disk electrode (RDE) studies corroborated the mechanism of a four-electron reduction of oxygen to water, emphasizing the catalyst's efficiency.

Keywords: cobalt catalyst; nanocellulose; polydopamine; electrochemistry; oxygen reduction reaction; clean energy; fuel cell

check for updates

Citation: Patwary, M.M.; Haque, S.; Szwedo, P.; Hasan, G.; Kondrapolu, R.S.; Watanabe, F.; KC, K.; Wang, D.; Ghosh, A. Exploring Enhanced Oxygen Reduction Reactions: A Study on Nanocellulose, Dopamine, and Cobalt Complex-Derived Non-Precious Electrocatalyst. Catalysts 2024, 14, 613. https:// doi.org/10.3390/catal14090613

Academic Editors: Carlo Santoro and Zhen Cheng

Received: 29 February 2024 Revised: 5 July 2024 Accepted: 5 September 2024 Published: 12 September 2024



Copyright: © 2024 by the authors. Licensee MDPI, Basel, Switzerland. This article is an open access article distributed under the terms and conditions of the Creative Commons Attribution (CC BY) license (https://creativecommons.org/licenses/by/4.0/).

1. Introduction

Fuel cells offer a viable alternative to the non-renewable energy sectors, such as petroleum and natural gas, by harnessing catalysts to accelerate the oxygen reduction reaction (ORR) crucial for their operation. Platinum (Pt) catalysts are favored for their high ORR efficiency and minimal overpotential [1]. Nevertheless, Pt's high cost poses significant economic challenges for widespread commercial adoption [2]. The escalating global demand for energy, driven by a growing population, higher living standards, and the ubiquity of portable devices, has led to an increased reliance on fossil fuels, which account for more than 85% of the energy used worldwide for stationary and automotive purposes [3]. This reliance on fossil fuels, which are depleting while also damaging the environment

Catalysts 2024, 14, 613 2 of 16

through contributions to global warming [4], highlights the urgent need for a shift toward alternative and renewable energy sources [5]. Efforts to utilize geothermal, hydro, wind, and solar power for energy production are underway, paralleled by research into batteries, fuel cells, and electrochemical supercapacitors for efficient energy storage [6–8]. Fuel cells stand out among alternative energy storage technologies, offering higher energy density compared to both flow batteries and lithium-ion batteries [9]. Although lithium-ion batteries boast portability, they are hindered by short lifespans, environmental pollution, and reduced effectiveness in extreme temperatures [10].

The interest in alternative energy systems is on the rise, with Proton Exchange Membrane Fuel Cells (PEMFCs) emerging as the leading technology in the field. PEMFCs are distinguished among fuel cell technologies for their superior energy conversion efficiency and power density, which ranges between 40% and 65% [11]. These fuel cells are also valued for their rapid startup and warmup times, ability to operate at relatively low temperatures (60 to 80 °C) [12], and their lightweight, compact design [13]. In PEMFCs, electricity is generated through an electrochemical reaction as protons move from the anode to the cathode. This setup includes a bipolar plate (flow field plate), a gas diffusion layer (GDL), and a catalyst layer (CL) at both the anode and cathode sides. At the anode, the hydrogen oxidation reaction (HOR) occurs, where hydrogen molecules are absorbed onto the catalyst layer, resulting in the detachment of electrons and the release of protons (H+). These electrons then make their way to the cathode via an external circuit, whereas the protons move through the membrane to reach the cathode. At this point, the oxygen reduction reaction (ORR) occurs, facilitating the production of electricity. The reactions within PEMFCs can be summarized as follows:

| Anode (HOR): | $2 H_2 \rightarrow 2 H^+ + 4 e^-$ | $E^{\circ} = 0.00 \text{ V vs. SHE}$ |
|-------------------|---------------------------------------|--------------------------------------|
| Cathode (ORR): | $O_2 + 4H^+ + 4e^- \rightarrow 2H_2O$ | E° = 1.23 V vs. SHE |
| Overall reaction: | $2H_2 + O_2 \rightarrow 2H_2O$ | SHE = Standard Hydrogen Electrode |

The primary challenge faced by Proton Exchange Membrane Fuel Cells (PEMFCs) is the need for high loadings of noble metal catalysts, such as platinum (Pt) and its alloys, at the cathode to accelerate the inherently slow ORR. These catalysts are essential for both the hydrogen oxidation reaction (HOR) and the ORR, with Pt and its alloys currently recognized as the most effective electrocatalysts due to their high catalytic activity, electronic conductivity, low overpotential, and outstanding stability [14–16]. However, the high cost of Pt significantly hinders the mass commercialization of PEMFCs [17,18]. This has led to efforts to develop non-precious metal catalysts (NPMCs) aimed at replacing Pt-based catalysts for the ORR, with recent research making considerable progress in improving the ORR performance of NPMCs, particularly those based on iron and cobalt [19]. A carbon-based bifunctional electrocatalyst offers a more efficient approach to constructing superior electrocatalysts. This is likely achieved by combining specific heteroatom doping and engineered carbon defects, which simultaneously have positive effects. To create porous B and N co-doped nanocarbon (also known as B, N-carbon) materials that are composed of interconnected cuboidal hollow nanocages with fine graphitization and ample carbon defects, a convenient strategy for facile construction has been developed. The resultant nanocarbon material, which combines carbon defects and B and N co-dopants, is an extremely reactive and long-lasting electrocatalyst for the ORR and the oxygen evolution reaction (OER) [20]. These advances have positioned NPMCs as viable alternatives to Pt and its alloys.

Polydopamine (PDA) has emerged as a novel, bio-inspired material attracting significant attention for its unique properties and applications in energy, the environment, and catalysis [21]. PDA, a synthetic polymer, demonstrates a strong affinity for solid substrates through chemical bonds and physical interactions, courtesy of its functional groups like amines, imines, and catechol [22,23]. Its excellent biocompatibility and surprising prop-

Catalysts **2024**, 14, 613 3 of 16

erties in terms of optics, electricity, and magnetism [21], along with similarities to mussel proteins, have spurred interest in its application across various domains, including coatings, environmental and catalytic applications, and energy storage and conversion [24–26]. The synthesis of N-doped carbon materials typically involves direct reactions with nitrogen precursors or the carbonization of nitrogen-containing polymers, with PDA polymerization offering a straightforward method for creating carbonaceous nanostructures [27–29].

Cellulose, the most abundant natural polymer, presents an opportunity for the synthesis of N-doped carbonaceous materials, including those containing metals [30]. Nanocellulose (NC), derived from cellulose, is noted for its environmental friendliness and excellent mechanical properties attributed to its nano-scale structure. This has led to its widespread application in engineering and functional materials [31]. NC, with dimensions in the nanometer range, is obtained from a variety of sources including plants, algae, and bacteria, and is characterized by its high surface area, mechanical strength, and biodegradability, making it suitable for high-performance energy devices [32]. The increasing demand for renewable energy solutions has catalyzed research into NC-based conductive materials. Despite the advancements, the stability of NPMCs remains a challenge, preventing them from being considered direct replacements for Pt/C catalysts in PEMFCs [19].

In this manuscript, we discuss the synthesis and application of a cobalt and nitrogendoped carbonaceous catalyst. The catalyst is synthesized by pyrolyzing a mixture of cobalt complex, NC, PDA, and urea at 500 °C under a nitrogen atmosphere, aiming to enhance the oxygen reduction reaction (ORR) efficiency in acidic fuel cells. We hypothesize that incorporating cobalt and nitrogen into the carbonaceous material matrix significantly boosts the electrocatalytic activity for the ORR in acidic environments, a critical aspect for fuel cell technology. The innovative aspect of our work lies in the synthesis strategy, which involves a unique blend of a well-dispersed cobalt complex, nanocellulose, and polydopamine, followed by pyrolysis with urea under an inert atmosphere. Characterization techniques such as SEM, XRD, and EDS have confirmed the presence of uniformly dispersed metal nanoparticles and an even elemental distribution. CV assessments demonstrated robust ORR activity, evidenced by a significant peak at 0.30 V against a reversible hydrogen electrode (RHE), particularly under acidic conditions and with uniformly layered electrodes. RDE experiments have further validated the four-electron reduction pathway of oxygen to water, highlighting the catalyst's potential in improving fuel cell performance.

2. Results and Discussions

2.1. Synthesis

The PPh₄⁺ salt of the cobalt complex and nanocellulose were mixed together in the presence of dopamine (hydrochloride salt), which was allowed to polymerize under an oxidative environment at a slightly elevated pH. The reaction mixture turned black, and a composite material precipitated, which is supposed to contain the cobalt complex along with nanocellulose coated with polydopamine. PDA plays a dual role: it is involved in the synthesis of the nanocellulose and cobalt complex nanocomposite, and it contains nitrogen atoms. Upon pyrolysis, these nitrogen atoms can dope the carbonaceous material, altering its structure and properties. After collecting the nanocomposite material postpolydopamine reaction, we added urea so that during pyrolysis, the carbonaceous material could be further doped with nitrogen atoms, which in turn can synergistically enhance ORR (oxygen reduction reaction) activities. NC contains several hydroxyl groups (-OH), which allow well dispersion and possible binding of the cobalt complex on its surface to enable uniform distribution of the catalytic site. NC also acts as a source of carbon when the catalyst is synthesized under pyrolysis. This unique synthesis route aims to achieve a homogeneous distribution of cobalt nanoparticles and nitrogen doping within the carbonaceous material matrix, hypothesized to synergistically improve the ORR performance by facilitating a more efficient four-electron reduction pathway of oxygen to water.

Catalysts **2024**, 14, 613 4 of 16

homogeneous distribution of cobalt nanoparticles and nitrogen doping within the carbonaceous material matrix, hypothesized to synergistically improve the ORR performance by facilitating a more efficient four-electron reduction pathway of oxygen to water.

2.2. Characterizations

2.2.1.2SEM and EDS

2.5EM integration was conducted to assess the morphology of the carbonaceous materials. The SEM integration presented in Figures and independent of the cobalt-dopad materials. Semination of the cobalt-dopad materials share figures have a supported by the semination of the cobalt-dopad materials. Semination of the cobalt-dopad materials share figures have a supported by the complete of the semination of the semination of the complete of the semination of the

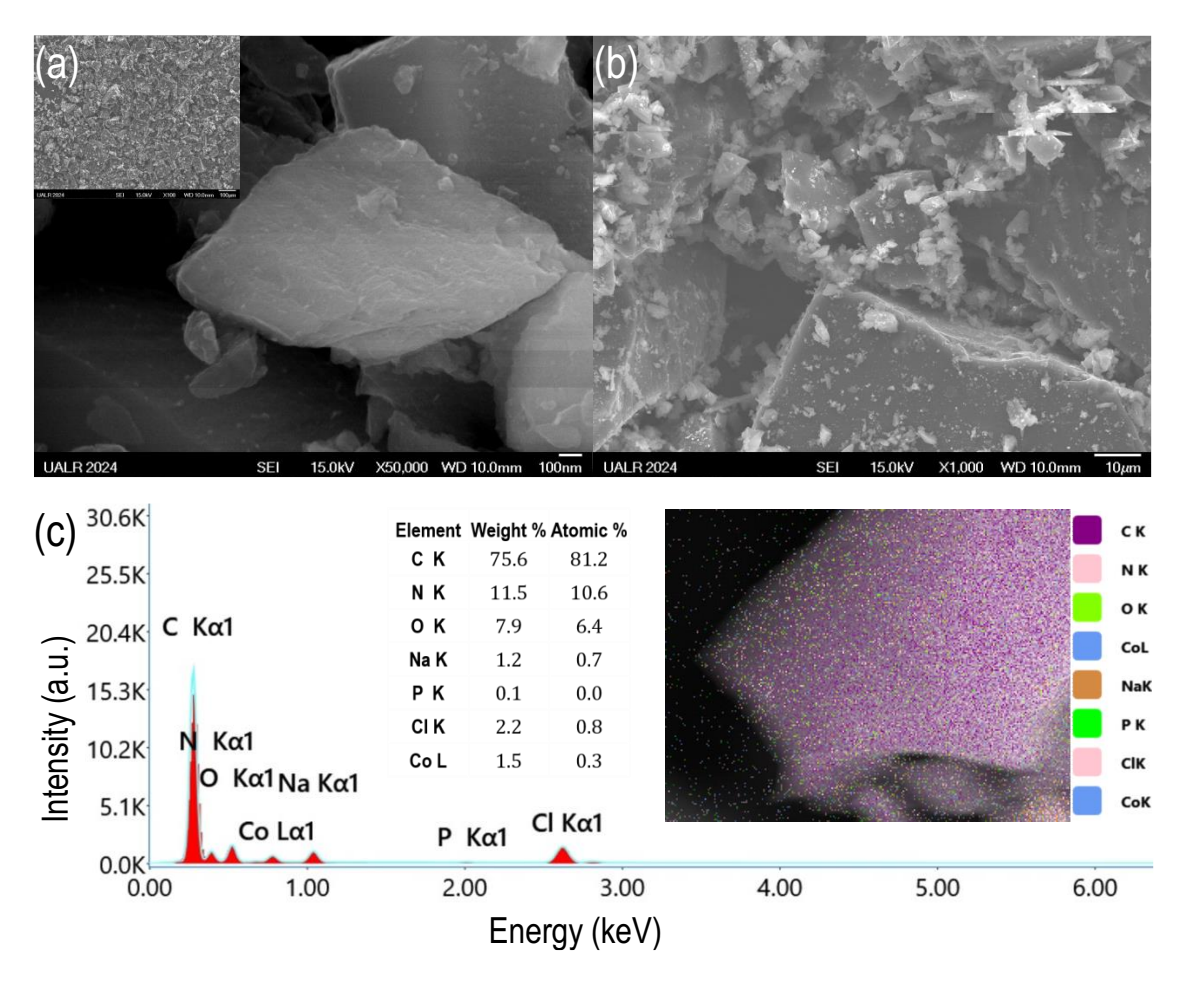


Figure 1. SEM images of cobalt-doped carbonaceous ORR catalytic material at **(a)** 50k magnification and **(b)** 1k magnification. **(c)** EDS spectra showing element mapping image of elements of carbonaceous material.

2.2.2. XRD

X-ray Diffraction (XRD) characterization was conducted to investigate the phase, structure, and crystallinity of the pyrolyzed material. The XRD patterns reveal the presence of cobalt oxides. The XRD pattern, depicted in Figure 2, confirms the crystalline nature of the sample. The diffraction peaks corresponding to Co_3O_4 were observed at 20 values of 27.33°, 31.66°, 45.43°, 56.45°, 66.23°, and 75.32°, which correspond to the (111), (220),

2.2.2. XRD

X-ray Diffraction (XRD) characterization was conducted to investigate the phase, 5 of 16 structure, and crystallinity of the pyrolyzed material. The XRD patterns reveal the presence of cobalt oxides. The XRD pattern, depicted in Figure 2, confirms the crystalline na-

(400), (422), (430), and (620) flatties, respectively 1935 in the valification peaks match with the CoTD 3d at abase and 1543° mobiles. The 323° and 775° 32° thick correspond to the that Co₃O₄ has the preferential orientation along the (220) plane. To further confirm the phase and match with the CoD database file number 1538531. The XRD spectrum suggests that chemical composition, the Raman spectrum was collected (Supplementary Information, Figure 51) has the preferential orientation along the (220) plane. To further confirm the phase and match with the CoD database file number 1538531. The XRD spectrum suggests that chemical composition, the Raman spectrum was collected (Supplementary Information, Figure 51) has the preferential orientation along the (220) plane. To further confirm the phase figure 51) has the preferential orientation along the (220) plane. To further confirm the phase of the supplementary Information, Figure 51) has the preferential orientation along the (220) plane. To further confirm the phase of the phase of the phase supplementary in the supplementary Information, Figure 51) the supplementary Information, Figure 51) the proposition of the past of the phase of the past of the phase of the past of

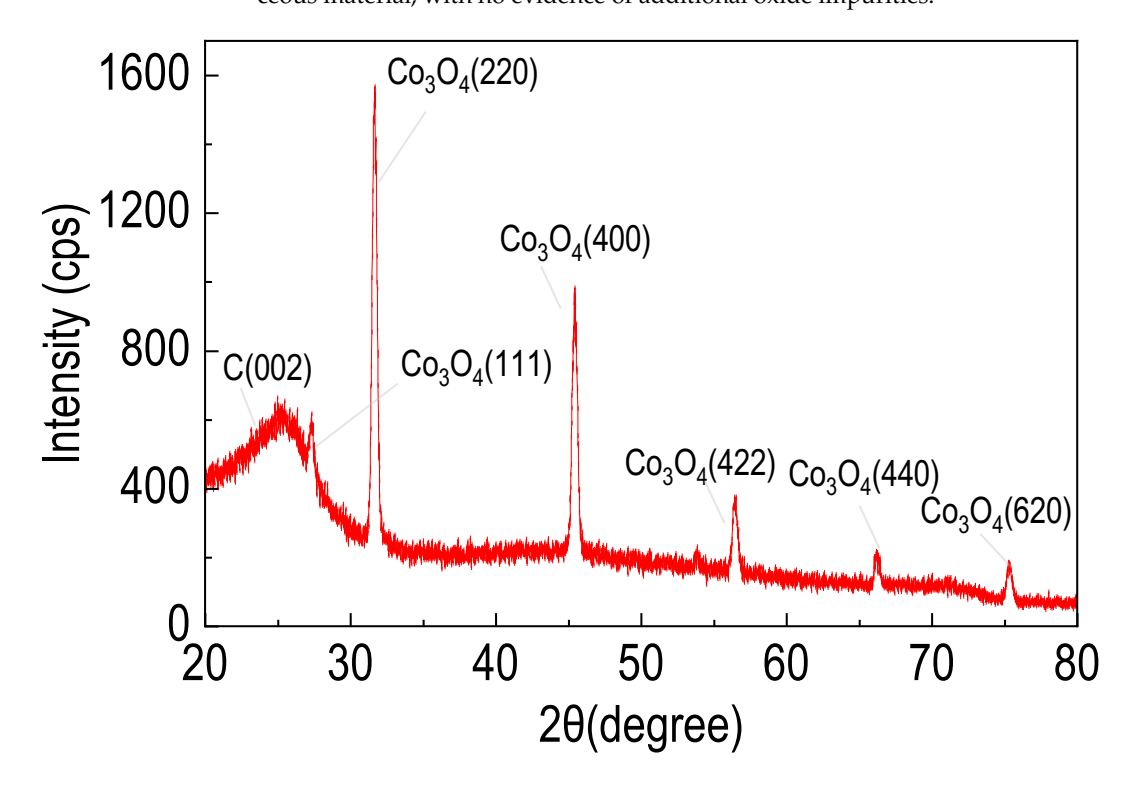


Figure 2. XRD pattern of pyrolyzed cobalt-doped carbonaceous ORR catalytic material. 2.2.3. XPS Study

X-ray Photoelectron Spectroscopy (XPS) analysis was performed on the pyrolyzed carbonaceous material to determine its surface elemental composition and the chemical states of carbon and cobalt (Co), which are crucial for its electrocatalytic activity. Initially, a survey scan of the material revealed the presence of major elements including C, N, O, and Co. During this survey, peaks were observed for both nitrogen and oxygen atoms. An oxygen peak was noted at approximately 532.6 eV, suggesting the presence of carbonyl oxygen in the sample [38]. A nitrogen peak was detected at 400.3 eV, indicating nitrogen doping in the carbonaceous material [39]. Nitrogen doping can enhance the material's properties, potentially altering its electronic structure, improving conductivity, or enhancing its catalytic properties. These modifications can be tailored for specific applications, such as energy storage devices, catalysis, sensors, and electronic devices. The C1s XPS peaks shown in Figure 3b reveal the chemical composition and bonding present in the carbonaceous material. The C1s spectrum exhibits distinct peaks at binding energies of

Catalysts 2024, 14, 613 6 of 16

284.8 eV, 286.0 eV, and 288.5 eV, corresponding to various carbon functional groups in the material [40]. The primary peak at 284.8 eV represents carbon atoms in sp3-hybridized structures prevalent in the sample. The peak at 286.0 eV is attributed to carbon atoms involved in C-O (carbon-oxygen) bonds, indicating the presence of oxygen-containing Catalysts 2024, 14, x FOR PEER REVIEWINGTIONAL FUNCTIONAL F

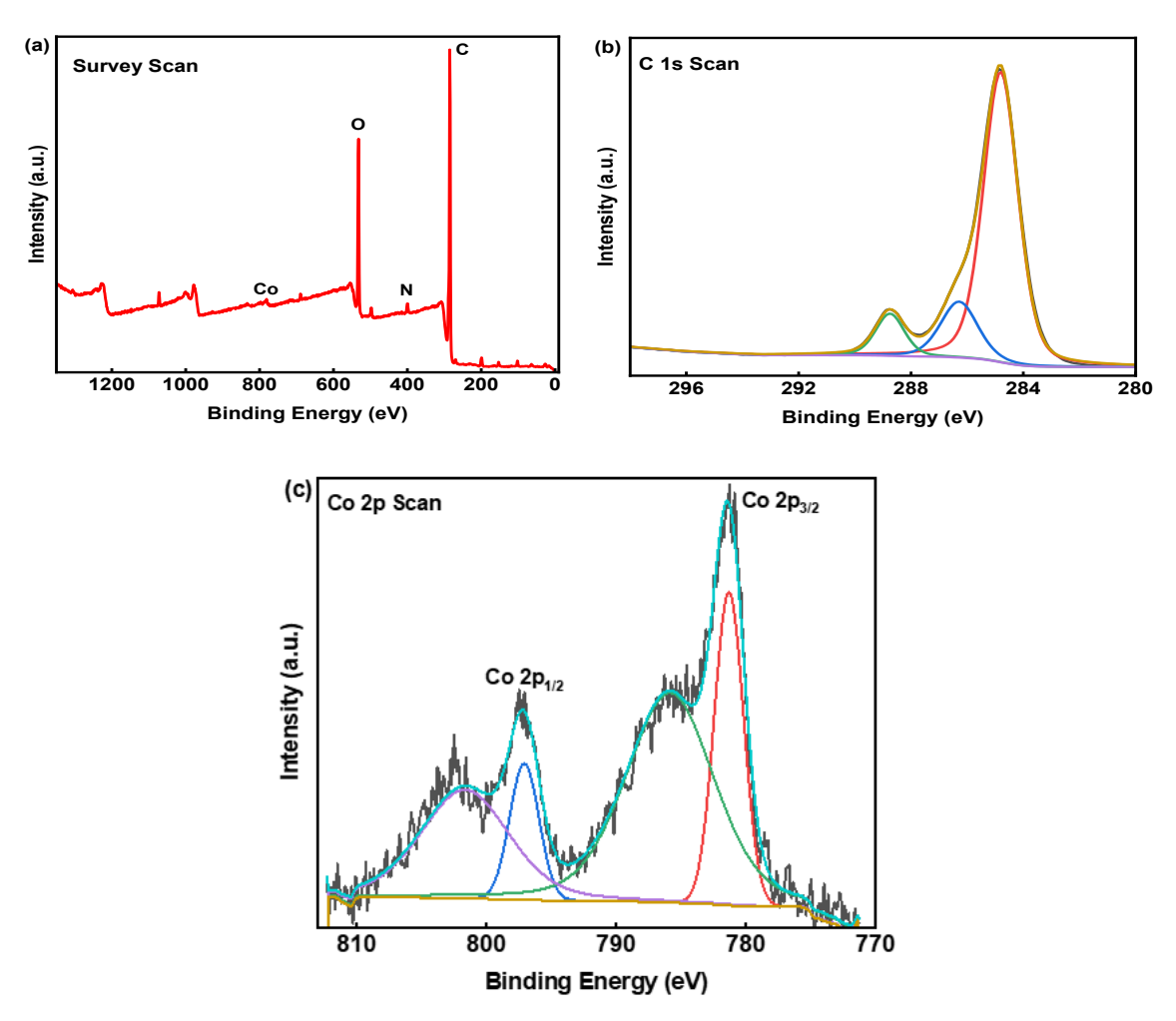


Figure 3. XIPS results of cobalt-dispedicarbonneous material: (a) survey sean, (b) C1 is narrow sean, and (c) Co2p narrow sean. [Fine red line means sum of speaks, the green line means background line and other color line represents peak fitting curve):

2.3. Circlient of the war the cobalt complex through Co 2p XPS scans unveiled two distinct penkaral epicted incligant a teach for fively pank the carried act of the carried act of the fively pank the carried act of the carried trithetoeketroenbitalatindetherseconderenkalinatedyste796eteletisasseciatad with the apostocornitaton. The Hart of the free formula presence of Ca(U) in the sample, axis disated the references 642-44 to ditionally satellite peaks nathing ing an argine of RR2 peeks and 7868 a Vervith of 15 ge expanses at in the twanty the typi2m1/2fendufing2m1/2 pevolatify: thre ceraphorate theraxis tence artiCo(11)844pportydy references of 55 the Given the XRP and Raman (Figure SP)/cesultaindicative/pothe Go Quand the Aseistin allowible thorresamples contains both Ca(H) and the (H) states eagle or he effect commy iges aboutly of the cobalt-doped carbonaceous material toward the ORR was initially examined a ship year Collian and Collian Res analysis is challenging the to their similar, peak positions, leaving room tor, both possibilities of rior XPS, data levels (1, 3, our standard stan 5, and 7) of a 0.1 M H₂SO₄ electrolyte solution, within a potential range of 0.0 V to 1.1 V (vs. RHE), under both O2- and Argon (Ar)-saturated conditions, as illustrated in Figure 4a,b. The results from the pH studies indicated that the catalyst displayed a sharper reduction peak in the electrolyte with a pH of 3 (Figure 4a), noting a significant reduction in the current at 0.30 V (vs. RHE) and 0.35 V (vs. RHE) at scan rates of 100 mV/s and 10

non-pyrolyzed complexes showed peak positions akin to those reported here [50], albeit identified in the Co(III) oxidation state. The presence of deprotonated amide peaks complicates the assignment further, as deprotonated amides significantly donate electrons to the metal. Despite the sample being subjected to a pyrolysis temperature of $500\,^{\circ}$ C, which typically leads to the decomposition of such complexes into metal oxides, it is conceivable that some original complex structures were retained, especially when polydopamine was involved. Pyrolysis is expected to break down the complex, as indicated by previous XRD and Raman analyses, potentially reducing Co(III) to Co(II) through the production of reducing gases during the process. The pyrolysis of our sample, enriched with nitrogen doping from dopamine, the amidomacrocyclic ligand, and urea, fundamentally altered the original complex structure. This transformation decomposed the metal complex and integrated metal and nitrogen into the matrix, potentially enhancing the material's oxygen reduction reaction (ORR) activities. This enhancement could be attributed to a synergistic interaction, with the metal or the nitrogen dopants serving as active sites for the ORR, illustrating the intricate relationship between material composition and electrocatalytic performance.

2.3. Cyclic Voltammetry (CV)

Electrochemical tests were conducted to evaluate the carbonaceous material's capability to electrochemically reduce oxygen in the oxygen reduction reaction (ORR). The most common method for efficiently evaluating the performance of a catalyst is to measure its half-wave potential $(E_{1/2})$. Assessing the ORR performance of a catalyst entails benchmarking against the ORR performance of a cutting-edge commercial Pt/C catalyst, typically featuring 20% Pt loading. The established average $E_{1/2}$ value of 0.84 \pm 0.03 V (vs. RHE) serves as the "Golden reference" for commercial Pt/C (with Pt 20 wt%), facilitating the assessment of other ORR catalysts in both acidic and alkaline electrolytes [51]. The electrocatalytic activity of the cobalt-doped carbonaceous material toward the ORR was initially examined using cyclic voltammetry (CV). CV measurements were taken at various scan rates (100 mV/s, 50 mV/s, 25 mV/s, and 10 mV/s) across different pH levels (1, 3, 5, and 7) of a 0.1 M H₂SO₄ electrolyte solution, within a potential range of 0.0 V to 1.1 V (vs. RHE), under both O_2 - and Argon (Ar)-saturated conditions, as illustrated in Figure 4a,b. The results from the pH studies indicated that the catalyst displayed a sharper reduction peak in the electrolyte with a pH of 3 (Figure 4a), noting a significant reduction in the current at 0.30 V (vs. RHE) and 0.35 V (vs. RHE) at scan rates of 100 mV/s and 10 mV/s,

Catalysts 2024, 14, x FOR PEER REPOSPECTIVELY, in the O₂-saturated environment. Additionally, a CV test was performed 17 under the same conditions but in an Ar-saturated environment to determine if the catalyst could reduce oxygen in its absence, where no peak was observed (Figure 4b).

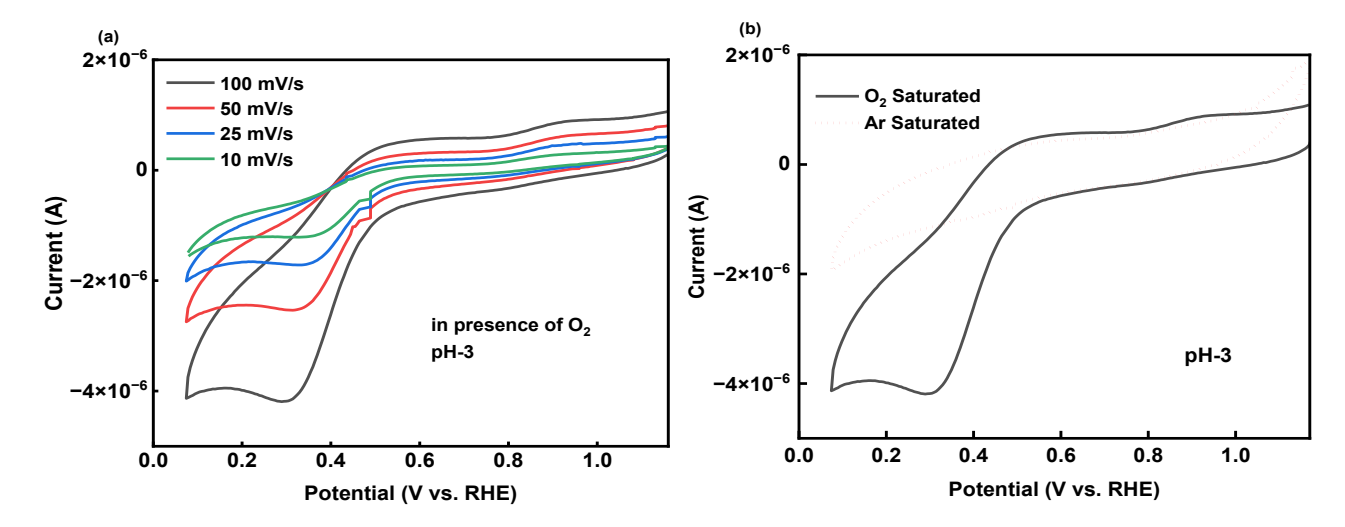


Figure 4. Cyclic voltammograms of pyrolyzed cobalt-doped carbonaceous material at pH 3 in **Figure 4.** Cyclic voltammograms of pyrolyzed cobalt-doped carbonaceous material at pH 3 in **(a)** O2-saturated 0.1 M H₂SO₄ and **(b)** Ar-saturated 0.1 M H₂SO₄, with v = 100 mV/s.

O2-saturated 0.1 M H₂SO₄ and **(b)** Ar-saturated 0.1 M H₂SO₄, with v = 100 mV/s.

2.3.1. Electrocatalyst Layer Studies

The oxygen reduction reaction (ORR) studies utilized different numbers of deposited layers (1, 3, 5, 7) on glassy carbon electrodes to investigate variations in the peak potential position and/or current density. Cyclic voltammetry tests were extended to seven layers,

Catalysts 2024, 14, 613 8 of 16

2.3.1. Electrocatalyst Layer Studies

The oxygen reduction reaction (ORR) studies utilized different numbers of deposited layers (1, 3, 5, 7) on glassy carbon electrodes to investigate variations in the peak potential position and/or current density. Cyclic voltammetry tests were extended to seven layers, revealing that electrodes with a greater number of uniform layers displayed a more pronounced reduction peak (Figure 5) in an oxygen-saturated solution. Notably, a distinct peak was recorded at 0.31 V (vs. RHE) for the electrode with seven layers in an O₂-saturated electrolyte solution at a scan rate of 100 mV/s. Incrementally adding layers of the carbonaceous material on the electrode surface resulted in a rise in current density [50], suggesting enhanced ORR activity. In comparison, the electrolyte solution saturated with argon exhibited a significantly weaker reduction peak across all layers relative to the O2saturated 0.1 M electrolyte solution. The peak's potential progressively shifted to lower values and its intensity decreased with a lesser number of layers. Adding layers potentially increases both the active sites and the electrical conductivity of the electrode, as more carbonaceous material enhances the overall ORR efficiency, leading to a higher current and shifts toward more positive potentials. The sample with seven layers showcased a sharper reduction peak, a result of the additional layers increasing the number of active sites and improving the electrical conductivity, thereby expanding the surface area. This ងីថ្លៃns with the observed trend, underscoring the importance of optimizing layer thickness

sites and improving the electrical conductivity, thereby expanding the surface area. This Catalysts 2024, 14, x FOR PEER REVIEW aligns with the observed trend, underscoring the importance of optimizing layer thickness for improved electrocatalytic performance.

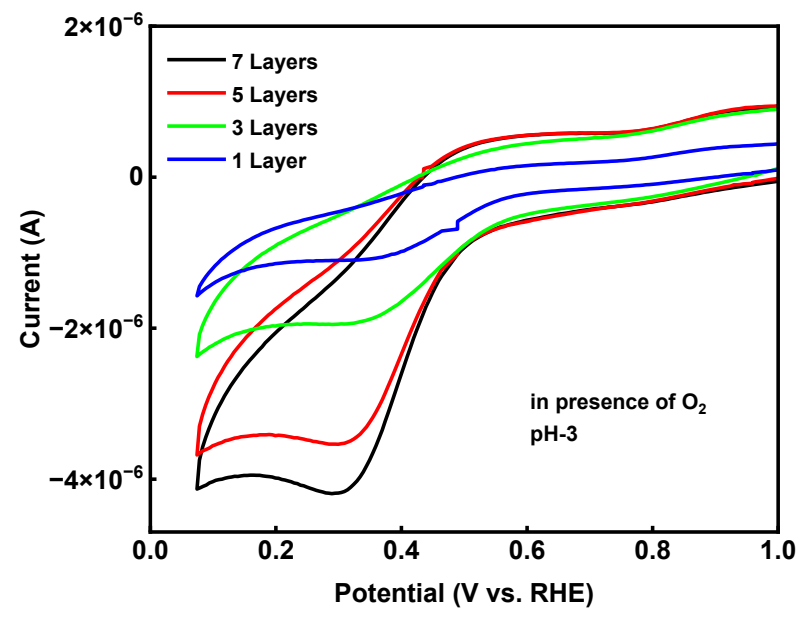


Figure 5. Cyclic voltammogram comparison for different layers in $0.1 \, \text{M} \, \text{H}_2 \text{SO}_4$ electrolyte solution, **Figure-51 Cyclic** (soltammogram comparison for different layers in $0.1 \, \text{M} \, \text{H}_2 \text{SO}_4$ electrolyte solution, with $v = 100 \, \text{mV/s}$. 2.3.2. Electrocatalyst pH and Stability Studies

2.3.2T Reperformance of the Stablisty was dealuated using cyclic voltammetry (CV) tests under various pH conditions (1, 3, 5, 7) in both O₂-saturated and Ar-saturated environments. In Figure 5a, the cobalt doped carbonaseous catalyst cyclic voltammetry (CV) tests in Figure 5a, the cobalt doped carbonaseous catalyst exhibited a pronounced reduction made at pH 3 in an oxygen (O₂)-saturated environment at a scan rate of 100 mV/s indicating ments. In Figure 6a, the cobalt-doped carbonaceous catalyst exhibited a pronounced reduction peak at pH 3 in an oxygen (O₂)-saturated environment at a scan rate of 100 mV/s, only modest reduction peaks were detected, suggesting a decrease in catalytic compared to pH 3. Remarkably, at pH 7, the catalyst showed no reduction peak, indicating environment, only modest reduction peaks were detected, suggesting a decrease in catalytic activity. Compared to pH 3. Remarkably, at pH 7, the catalyst showed no reduction peak, indicating environment, only modest reduction peaks were detected, suggesting a decrease in catalyst significant drop in activity in less acidic environments. This trend confirms that the lytic activity compared to pH 3. Remarkably, at pH 7, the catalyst showed no reduction catalyst selficiency is maximized in more acidic conditions. In contrast, the CV tests peak, indicating a significant drop, in activity in less acidic environments. This trend confirms that the catalyst selficiency is maximized in more acidic conditions. In contrast, the any pH level, with only a very slight peak observable for pH 1, 3, and 5 (Figure 6b), and again, no peak was detected from pH 7 upwards. The absence of significant activity in the Ar-saturated tests across all pH levels emphasizes the catalyst's specificity for the oxygen reduction reaction in acidic media, highlighting its potential application in

environments where efficient ORR activity is critical. The electrochemical stability study

again, no peak was detected from pH 7 upwards. The absence of significant activity in the Ar-saturated tests across all pH levels emphasizes the catalyst's specificity for the oxygen reduction reaction in acidic media, highlighting its potential application in environments where efficient ORR activity is critical. The electrochemical stability study aims to examine the stability of the carbonaceous material through cyclic voltammetry (CV) measurements. The stability of the catalyst is an important requirement for its operation. It has been recently discovered that ensuring the long-term stability of the Membrane/Electrode Assembly (MEA) is crucial for commercializing fuel cells. An investigation through XPS data has revealed that the amount of fluorine atoms in the fuel cell gradually decreases over time due to the degradation of Nafion [52]. In this study, we investigated the chemical stability of our material up to 500 cycles at pH 3 under an oxygen (O₂)-saturated environment at a scan rate of 100 mV/s with a voltage window from 0.0 V to 1.1 V (vs. RHE). During the 500 cycles, drop-cast working electrode materials experienced a significant loss during the experiment, and it resulted in a consequential decrease in the reduction peak (Figure 6c). This degradation of active materials on the electrode surface may have resulted from irreversible reactions in the electrolyte. The effect of binders can be another factor for this kind of decrease in reduction peak. We used Nafion as a binder due to its high ionic conductivity and chemical stability. However, Nafion tends to swell in certain electrolytes or solvent environments, which can compromise the stability and electrocatalytic performance of the material over time. Although Nafion is chemically stable, its hydrophobic nature may impede the wetting of electrode surfaces, affecting electrochemical reactions and leading to reduced performance, particularly in aqueous environments. We have planned to experiment with different electrolytes and binders to improve the stability of the pyrolyzed cobalt-doped carbonaceous material.

2.3.3. Rotating Disk Electrode (RDE)

RDE studies were conducted on the carbonaceous material to determine the number of electrons involved in the ORR. In acidic conditions, oxygen can be reduced to water in a four-electron process. However, sometimes, oxygen can be reduced to hydrogen peroxide through a two-electron exchange process. Even though the reduction of oxygen to hydrogen peroxide is also an ORR process, generating peroxide is undesirable since it has an oxidative character that degrades the catalyst, which decreases its ORR activity. RDE tests were performed by rotating a drop-cast glassy carbon electrode at different rotation speeds ($\omega = 400$ to 2500 rpm) with a 10 mV/s scan rate in O₂-saturated 0.1 M H₂SO₄ (Figure 7a).

To calculate the number of electrons involved in an electrochemical process, the convective movement between the analyte solution and the electrode surface is related using the Koutecky–Levich equation. The Levich current (J_{lev}) is calculated using the equation $J_{lev} = 0.620 n F C D^{2/3} \omega^{1/2} v^{-1/6}$, where n is the number of electrons transferred, F is the Faraday constant, C is the molar concentration of the analyte, D is the diffusion coefficient of O_2 , ω is the angular rotation rate of the electrode, and ν is the kinematic viscosity of the solution. The kinetic current (J_k) and the observed limiting current (J_{lim}) from the experimental RDE data are used to construct the Koutecky–Levich equation. The slope of J_{lev} is obtained by plotting the graph between J_{lim}^{-1} and $\omega^{-1/2}$.

$$1/J_{lim} = 1/J_{lev} + 1/J_{k}$$

where J_{lim} is the limiting current density, J_{lev} is the Levich current, and J_k is the kinetic current

From the slope of the K-L plot, the number of electrons involved in the oxygen reduction mechanism is determined using the equations mentioned above. According to the calculated results, the catalyst performs the ORR through a 3.58 electron process at pH 3, which matches the theoretical n = 4 value (Figure 7b).

electrocatalytic performance of the material over time. Although Nafion is chemically stable, its hydrophobic nature may impede the wetting of electrode surfaces, affecting electrochemical reactions and leading to reduced performance, particularly in aqueous environments. We have planned to experiment with different electrolytes and binders to im-¹ of ¹⁶ prove the stability of the pyrolyzed cobalt-doped carbonaceous material.

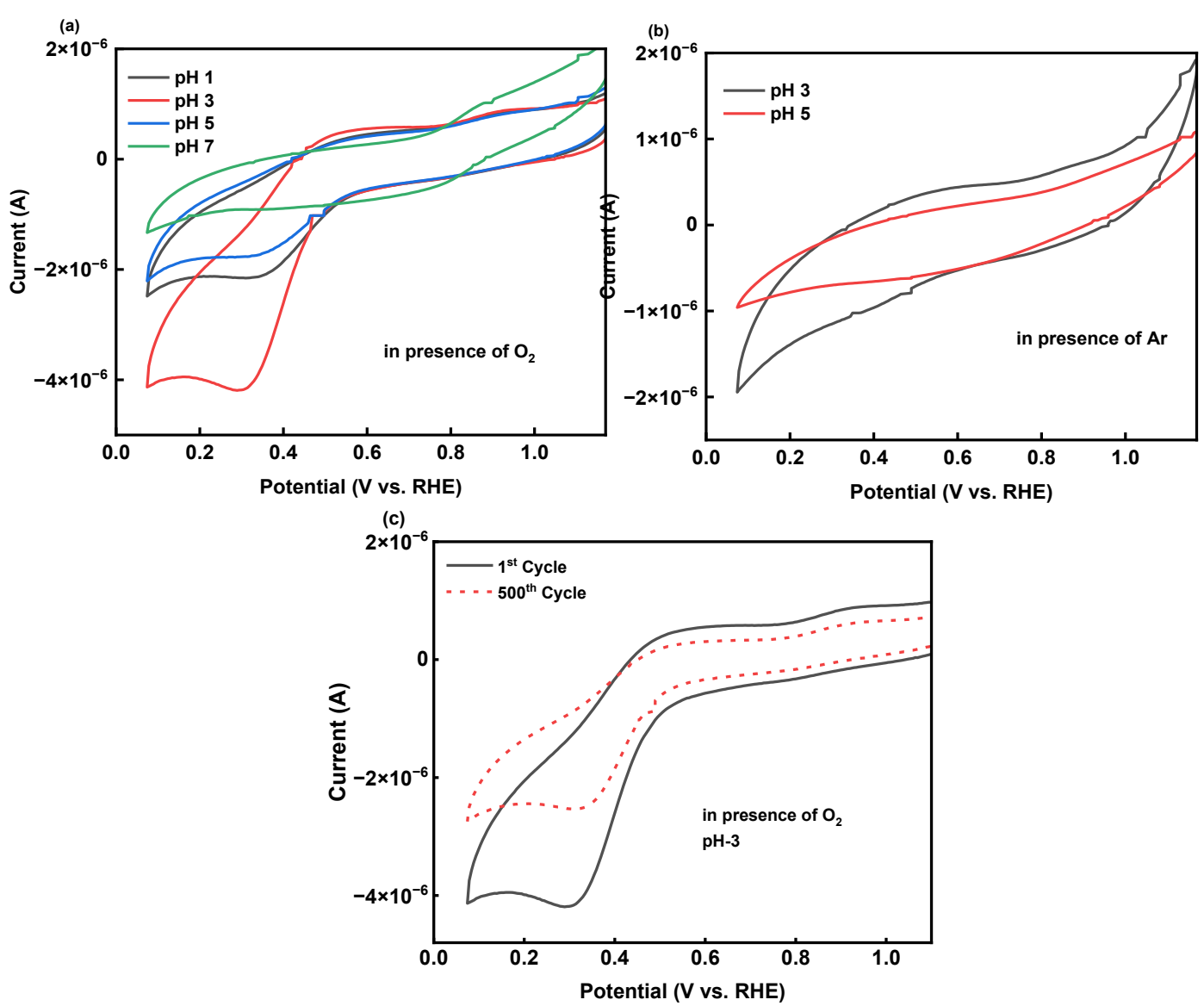


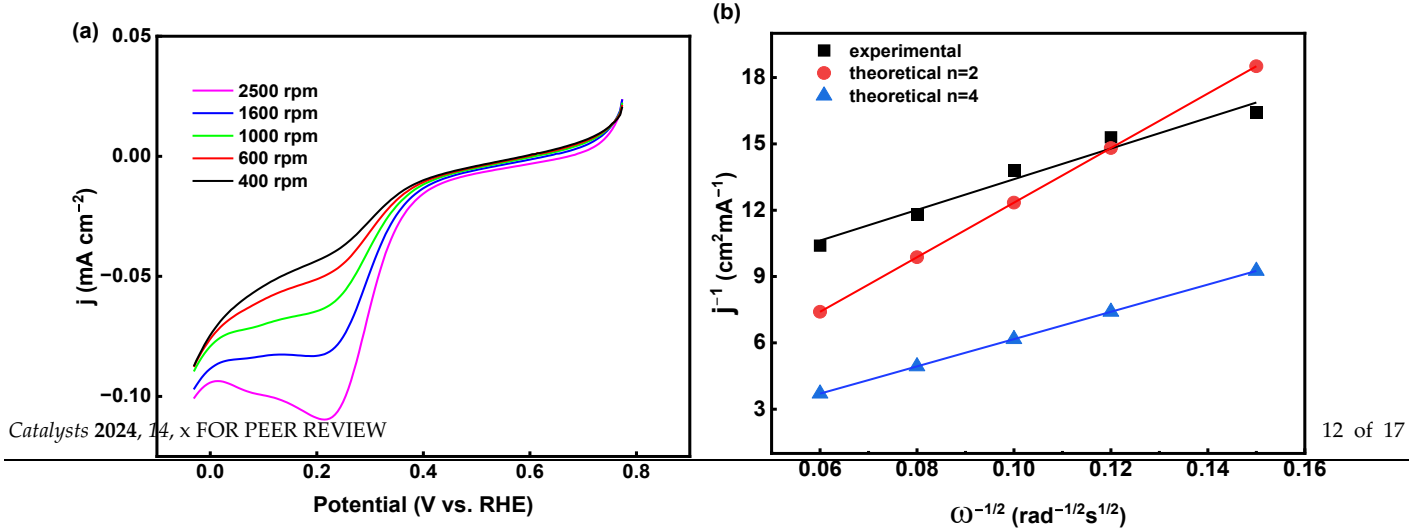
Figure 6. Cyclic voltammograms of cobalt-doped carbonaceous catalyst with different pH values in (a) OF igure the Cyclic work of the Cyclic work o

2.3.3. Rotating Disk Electrode (RDE) 2.4. Proposed Mechanism

RDE studies were conducted on the carbonaceous material to determine the number. The RDE studies provide clear evidence that the material catalyzes the oxygen reduction for the ORR. In acidic conditions, oxygen can be reduced to water in the reaction (ORR) through a four-electron mechanism in acidic environments, a conclusion a four-electron process. However, sometimes, oxygen can be reduced to hydrogen peroxsupported by electrochemical analyses at pH 3. This efficient four-electron pathway is ide through, a two-electron exchange process. Even though the reduction of oxygen peroxide is also an ORR process, generating her oxide is undesirable since it has species within the catalytic material, indicating that these Co centers could serve as the an oxidative character that degrades the catalyst, which decreases its ORR activity. RDE critical active sites for the ORR, with molecular O2 initially binding to them. Although tests were performed by rotating a drop-cast glassy carbon electrode at fifteent rotation with speeds (\omega=400 to 2500 rpm) with a 10 mV/s scan rate in O2-saturated 0.1 M H2SO (Figure 7a). effectiveness of these active sites for the ORR process. Interestingly, during the ORR, the Co center temporarily reaches a higher oxidation state when it first binds with an O2 molecule. The reaction ends with the reduction of O2 to water, which interestingly brings the Co center back to its original oxidation state, either II or III, thus completing the catalytic cycle in the challenging environment of acidic conditions. This reversible oxidation-reduction

11 of 17

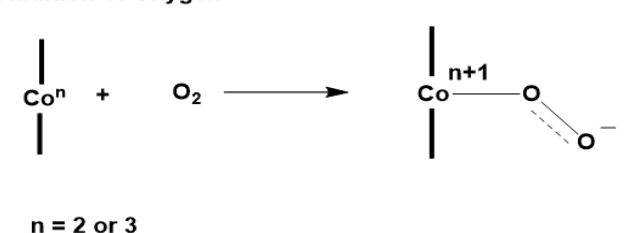
cycle highlights the durability and effectiveness of the catalytic process, pointing out the catalyst's potential as an excellent catalyst for ORRs [53,54].



cycle in the challenging environment of acidic conditions. This reversible oxidation—re-Flautron (a) RD highlighted the day and shifty and overteeth white Openham and the properties of the stand by the properties of the same special properties of

Acidic to neutral medium

(a) Addition of Oxygen



ess, the conelated using he equation the Faraday ient of O_2 , ω the solution. mental RDE obtained by

the kinetic

(b) Reduction of Oxygen

 Co^{-} + $4H^{+}$ + $4e^{-}$ Co^{n} + $4H_{2}O$ except representation in the case at pH 3,

Figure 8. Proposed mechanism for ORR using cobalt-daped carbonaceous material. 2.4. Proposed Mechanism

Materials and Methods Materials and Methods vide clear evidence that the material catalyzes the oxygen reducreaction (ORR) through a four-electron mechanism in acidic environments, a conclusion supported by used in the critical unvelve sourced from is latricle aftermisele Coopst Julian MOJUBAT BATTERBURGE TO THE THE THE THE THE TEACHER WERE THE TRANSPORT OF THE THE THE TRANSPORT OF THE TRANSP usbeeles acitified total envision of the control of SEINABURIES GREIFER RECEVEE THE PROPERTY OF THE SECOND FOR THE SEC anieni nekaturus perintuk aliku karan kara SPECERESESPY NEEDS PROPRETED AND VARIOUS REPORTED SERVICES FOR THE PROPRETED FOR THE MUNITER YANGODERINE DE BENES ET RECEPTORISATION OF A POST AND A PO wang dali perci Miriniste, and the rediction of the worder. White interest in a ben zenier materiali was determined using 12-rayh Phat selagtron. Spectroscopy i NPST any de Thermo Scientific (Waltham, MA, USA) K-Alpha instrument with Al K α radiation. Cyclic voltammetry (CV) experiments to assess electrocatalytic activity were conducted with a Pine Instruments potentiostat (Raleigh, NC, USA) in a 0.1 M H2SO4 solution. pH and layer deposition studies also utilized the Pine Instruments potentiostat in a 0.1 M H₂SO₄ solution, Pyrolysis was performed in an MTI Corporation (GSL-1100X, Richmond, CA, USA)

Catalysts 2024, 14, 613 12 of 16

> (Waltham, MA, USA) K-Alpha instrument with Al Kα radiation. Cyclic voltammetry (CV) experiments to assess electrocatalytic activity were conducted with a Pine Instruments potentiostat (Raleigh, NC, USA) in a 0.1 M H₂SO₄ solution. pH and layer deposition studies also utilized the Pine Instruments potentiostat in a 0.1 M H₂SO₄ solution. Pyrolysis was performed in an MTI Corporation (GSL-1100X, Richmond, CA, USA) high-temperature furnace. Oxygen and argon gases for the research were supplied by Airgas, and deionized water was used for all washing procedures.

3.2. Synthesis of Cobalt-Doped Carbonaceous Material

The cobalt complex of the amidomacrocyclic ligand was synthesized using a previously published synthetic method with slight modifications [55]. Initially, the lithium salt of the cobalt complex was synthesized. Tetraphenylphosphonium (PPh₄⁺) salts of inorganic or metalloorganic anions are commonly utilized due to their ease of crystallization. Consequently, the countercation was switched from lithium (Li⁺) to tetraphenylphospho-Catalysts 2024, 14, x FOR PEER REVIEW (PPh₄⁺) by dissolving 300.0 mg of the initial cobalt complex in deionized water and incrementally adding a 3.0 M solution of tetraphenylphosphonium chloride (PPh₄Cl). The resulting precipitate was collected through filtration, and the product was subsequently dried under vacuum for 5-6 h.

> Next, 120.0 mg of nanocellulose was combined with the newly synthesized cobalt complex in deionized water, and the pH of the solution was adjusted to 8. To facilitate binding, 3380 mg of dopamine hydrochloride (DA HCl) was introduced to the mixture. This mixture was the eplated another helptate distinctly gently for 12ch in 12ch en airen alle w tat policitopalvitoparniation miatan oxial ativoxio dynnericationerization. Afteensa rafithe cont, tehetsomeratsollectechbectedriadlutridet under machinallyFi2Ally/12A.@.ofngref (CFJ (CFQ)Ny@) firms yi group got and lacked do the total as a first learning the first property of the first learning the Pigunder) wand avvolutsis/ad 500s of 500le Caunide genitatoges platenes phere.

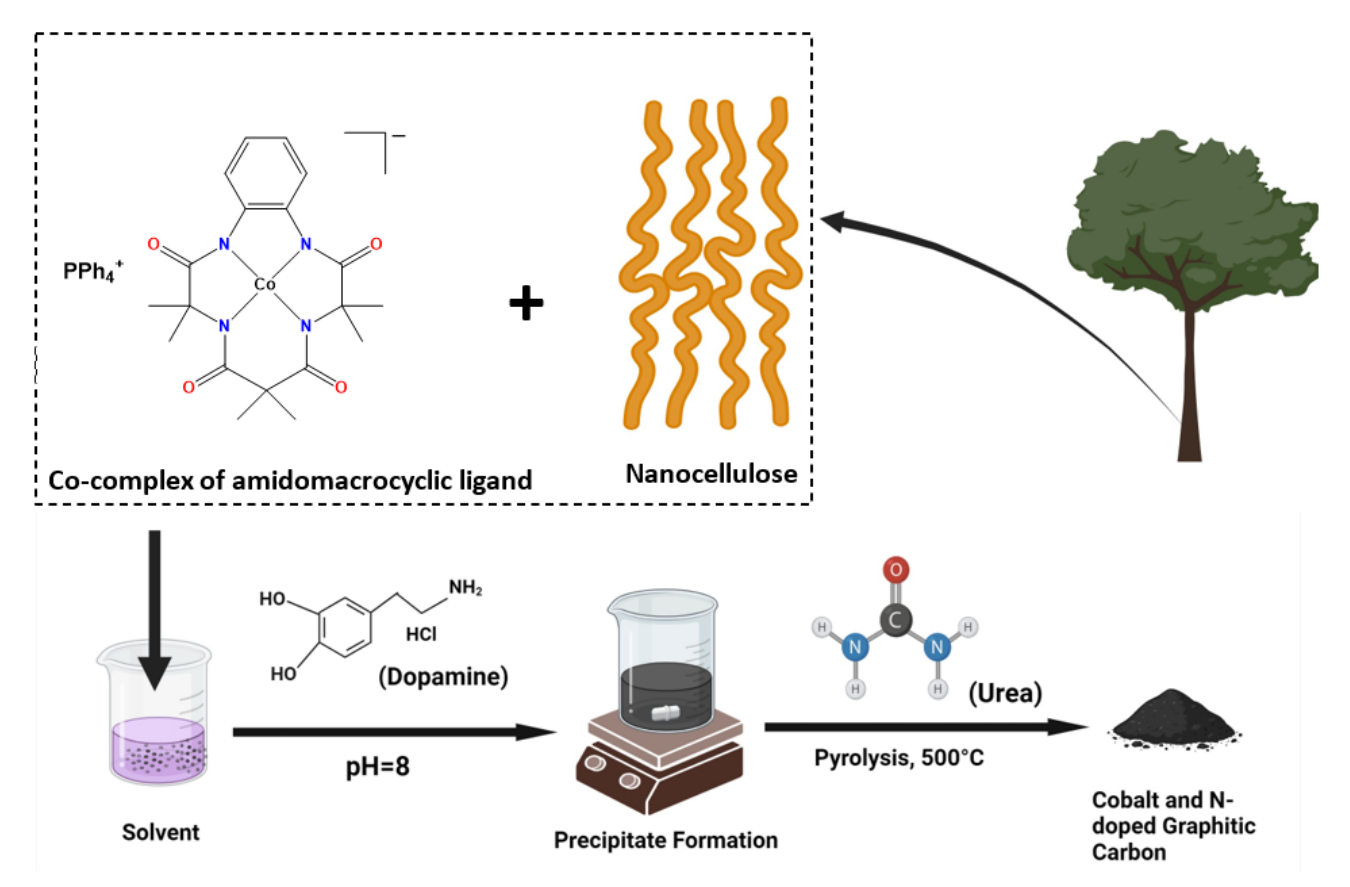


Figure 9. Schemattic illustration of the synthesis of the cobalt-doped carbonaceous material catalyst for enhanced ORR activity:

3.3. Electrochemical Studies

A potentiostat facilitated the cyclic voltammetry (CV) experiments. For these tests, a glassy carbon electrode from BASi Research Product (Lafayette, IN, USA) served as the working electrode. The reference electrode, Ag/AgCl, and the counter electrode, a plati-

3.3. Electrochemical Studies

A potentiostat facilitated the cyclic voltammetry (CV) experiments. For these tests, a glassy carbon electrode from BASi Research Product (Lafayette, IN, USA) served as the working electrode. The reference electrode, Ag/AgCl, and the counter electrode, a platinum wire, were sourced from Pine Instruments and BASi Research Product, respectively. The setup included a 100 mL glass vial as the electrochemical cell, sealed with a three-holed stopper. Concentrated sulfuric acid was diluted to a 0.1 M H_2SO_4 solution, yielding a predicted pH of 1.0. CV measurements spanned potential ranges from 0.0 V to 1.1 V (vs. RHE) at various scan rates. These electrochemical studies were conducted at an ambient temperature (25 °C) using a freshly prepared 0.1 M H_2SO_4 electrolyte solution. An O_2 -saturated environment was established for the experiments by bubbling oxygen gas through the electrolyte solution for at least one hour prior to testing, a condition that was maintained during the experiments. To evaluate the activity of the synthesized carbonaceous material, the electrolyte solution was deoxygenated with argon (Ar) gas. Throughout this study, all potential values are reported relative to the reversible hydrogen electrode (RHE), as per the specified expression.

$$E_{RHE} = E_{Ag/AgCl} + E^{\circ}_{Ag/AgCl} + 0.059pH$$

 E_{RHE} is the potential versus RHE in this equation. The potential measured against the Ag/AgCl reference electrode is denoted by $E_{Ag/AgCl}$. The standard electrode potential of the Ag/AgCl reference electrode in 0.1 M H_2SO_4 is $E^{\circ}_{Ag/AgCl}$.

Layer and pH studies were carried out by performing CV tests at different scan rates ranging from 0.0~V to 1.1~V (vs. RHE) in both O_2 - and Ar-saturated $0.1~M~H_2SO_4$ or buffered electrolytes.

3.4. Electrode Preparation

A homogeneous catalyst suspension was prepared by dissolving 5 mg of the catalyst in 5 mL of methanol, achieving a 1:1 weight/volume (w/v) ratio. To ensure uniformity, the mixture was sonicated for 10 min. Subsequently, after sonication, 40 μ L of Nafion solution (5 wt.%) was added to the homogeneous suspension. The surface of the glassy carbon electrode was initially polished with a 0.05 μ m alumina slurry and then thoroughly rinsed with deionized water. Following this, 20 μ L of the catalyst suspension was drop-cast onto the polished glassy carbon electrode surface and allowed to dry under vacuum. For the electrocatalyst layer studies, the procedure was similar to that used for cyclic voltammetry (CV) testing; however, 10 μ L of the catalyst suspension was drop-cast onto the glassy carbon surface for each layer, with each application followed by drying under vacuum.

4. Conclusions

A cobalt complex along with nanocellulose, polydopamine, and urea composite material was synthesized for use as a cathode catalyst in fuel cell applications. Characterizations of the metal-doped carbonaceous material were conducted using SEM, EDS, XRD, and XPS. SEM analysis revealed the morphology and nanostructure of the material, with some agglomeration observed. EDS confirmed the uniform distribution of elements within the carbonaceous material, while XRD identified the crystalline structures of ${\rm Co}_3{\rm O}_4$ and ${\rm Co}_3{\rm O}_4$. The electrocatalytic behavior of the cobalt-doped carbonaceous material toward the oxygen reduction reaction (ORR) in acidic media was investigated through cyclic voltammetry (CV) and rotating disk electrode (RDE) techniques. CV analysis demonstrated the ORR activity of the Co-doped carbonaceous material across different pH levels, with a pronounced peak at pH 3, showing a peak potential of 0.30 V (vs. RHE) in an oxygen-saturated 0.1 M H₂SO₄ electrolyte solution at a scan rate of 100 mV/s. This indicates the material's capability for ORRs. Further pH and layering studies were conducted using the CV system. RDE measurements determined that the cobalt complex catalyzes the ORR via a four-electron pathway. These findings offer new insights that could be beneficial for various applica-

tions, including acidic fuel cells, electrocatalytic reduction processes, batteries, biosensors, and supercapacitors.

Supplementary Materials: The following supporting information can be downloaded at: https://www.mdpi.com/article/10.3390/catal14090613/s1, Figure S1: Raman spectrum of pyrolyzed cobalt-doped carbonaceous ORR catalytic material. References [56–58] are cited in the Supplementary Materials.

Author Contributions: M.M.P., S.H., P.S., G.H., R.S.K., F.W., K.K., D.W. and A.G. contributed to the experimental design and data interpretation. A.G. conceived the study and experimental design. M.M.P., S.H., F.W., K.K., P.S. and A.G. contributed to the experimental design and wrote the manuscript. All authors have read and agreed to the published version of the manuscript.

Funding: This study was financially supported by the National Science Foundation (grant no. 2223984). A.G. would like to thank NSF for funding the research.

Data Availability Statement: All data are kept in the corresponding laboratories and are available upon request.

Acknowledgments: A.G. would also like to thank the UA-Little Rock Signature Experience for partially funding the research. The authors would like to thank The Center for Integrative Nanotechnology Science (CINS) at UA-Little Rock for all their help and support. The authors would also like to acknowledge the use of www.BioRender.com to draw the schematic illustrations.

Conflicts of Interest: The authors declare no conflicts of interest.

References

- Chhetri, B.; Parnell, C.; Wayland, H.; Rangumagar, A.; Kannarpady, G.; Watanabe, F.; Albkuri, Y.; Biris, A. Chitosan-Derived NiO-Mn₂O₃/C Nanocarbonaceouss as Non-Precious Catalysts for Enhanced Oxygen Reduction Reaction. *Chem. Sel.* 2018, 3, 922–932. [CrossRef]
- 2. Parnell, C.; Chhetri, B.; Brandt, A.; Watanabe, F.; Alsudani, Z.; Mudalige, T.; Biris, A. Polydopamine-Coated Manganese Complex/Graphene Nanocarbonaceous for Enhanced Electrocatalytic Activity Towards Oxygen Reduction. *Sci. Rep.* **2016**, *6*, 31415. [CrossRef] [PubMed]
- 3. Jaouen, F.; Proietti, E.; Lefevre, M.; Chenitz, R.; Dodelet, J.-P.; Wu, G.; Chung, H.T.; Johnston, C.M.; Zelenay, P. Recent advances in non-precious metal catalysis for oxygen-reduction reaction in polymer electrolyte fuelcells. *Energy Environ. Sci.* **2011**, *4*, 114–130. [CrossRef]
- 4. Shafiee, S.; Topal, E. When will fossil fuel reserves be diminished? Energy Policy 2009, 37, 181–189. [CrossRef]
- 5. Parnell, C.M.; Chhetri, B.P.; Mitchell, T.B.; Watanabe, F.; Kannarpady, G.; RanguMagar, A.B.; Zhou, H.; Alghazali, K.M.; Biris, A.S.; Ghosh, A. Simultaneous Electrochemical Deposition of Cobalt Complex and Poly(pyrrole) Thin Films for Supercapacitor Electrodes. *Sci. Rep.* **2019**, *9*, 5650. [CrossRef]
- 6. Dicks, A.L. The role of carbon in fuel cells. *J. Power Sources* **2006**, 156, 128–141. [CrossRef]
- 7. Wang, D.; Haque, S.; Williams, T.; Karim, F.; Hariharalakshmanan, R.K.; Al-Mayalee, K.H.; Karabacak, T. Cyclic voltammetry and specific capacitance studies of copper oxide nanostructures grown by hot water treatment. MRS Adv. 2023, 9, 979–985. [CrossRef]
- 8. Haque, S.; Wang, D.; Ergul, B.; Basurrah, A.O.M.; Karabacak, T. Effect of sandblasting and acid surface pretreatment on the specific capacitance of CuO nanostructures grown by hot water treatment for supercapacitor electrode applications. *Nanotechnology* **2024**, 35, 335403. [CrossRef]
- 9. Ning, F.; He, X.; Shen, Y.; Jin, H.; Li, Q.; Li, D.; Li, S.; Zhan, Y.; Du, Y.; Jiang, J.; et al. Flexible and Lightweight Fuel Cell with High Specific Power Density. *ACS Nano* **2017**, *11*, 5982–5991. [CrossRef]
- 10. Hou, J.; Shao, Y.; Ellis, M.W.; Moore, R.B.; Yi, B. Graphene-based electrochemical energy conversion and storage: Fuel cells, supercapacitors and lithium ion batteries. *Phys. Chem. Chem. Phys.* **2011**, *13*, 15384–15402. [CrossRef]
- 11. Basile, A.; Ghasemzadeh, K. *Current Trends and Future Developments on (Bio-) Membranes*; Elsevier: Amsterdam, The Netherlands, 2019. Available online: https://www.sciencedirect.com/book/9780128241035 (accessed on 5 December 2023).
- 12. Goswami, C.; Hazarika, K.K.; Bharali, P. Transition metal oxide nanocatalysts for oxygen reduction reaction. *Mater. Sci. Energy Technol.* **2018**, *1*, 117–128. [CrossRef]
- 13. Cigolotti, V.; Genovese, M.; Fragiacomo, P. Comprehensive Review on Fuel Cell Technology for Stationary Applications as Sustainable and Efficient Poly-Generation Energy Systems. *Energies* **2021**, *14*, 4963. [CrossRef]
- 14. Zhang, J. PEM Fuel Cell Electrocatalysts and Catalyst Layers; Springer: Berlin/Heidelberg, Germany, 2008. [CrossRef]
- 15. Stamenkovic, V.R.; Fowler, B.; Mun, B.S.; Wang, G.; Ross, P.N.; Lucas, C.A.; Markovic, N.M. Improved Oxygen Reduction Activity on Pt₃Ni(111) via Increased Surface Site Availability. *Science* **2007**, *315*, 493–497. [CrossRef] [PubMed]

16. Wang, Q.; Li, Y.; Liu, B.; Dong, Q.; Xu, G.; Zhang, L.; Zhang, J. Novel recyclable dual-heterostructured Fe₃O₄@CeO₂/M (M = Pt, Pd and Pt–Pd) catalysts: Synergetic and redox effects for superior catalytic performance. *J. Mater. Chem. A* **2015**, *3*, 139–147. [CrossRef]

- 17. Gewirth, A.A.; Thorum, M.S. Electrochemical CO₂ reduction catalyzed by a cobalt salophen complex. *Inorg. Chem.* **2010**, *49*, 3557–3566. [CrossRef]
- 18. Tollefson, J. Climate change: The Earth is warming faster than expected. Nat. News 2010, 464, 1262–1264. [CrossRef]
- 19. Banham, D.; Ye, S.; Pei, K.; Ozaki, J.; Kishimoto, T.; Imashiro, Y. A review of the stability and durability of non-precious metal catalysts for the oxygen reduction reaction in proton exchange membrane fuel cells. *J. Power Sources* 2015, 285, 334–348. [CrossRef]
- 20. Sun, T.; Wang, J.; Qiu, C.; Ling, X.; Tian, B.; Chen, W.; Su, C. B, N Codoped and Defect-Rich Nanocarbon Material as a Metal-Free Bifunctional Electrocatalyst for Oxygen Reduction and Evolution Reactions. *Adv. Sci.* **2018**, *5*, 1800036. [CrossRef]
- 21. Liu, Y.; Ai, K.; Lu, L. Polydopamine and its derivative materials: Synthesis and promising applications in energy, environmental, and biomedical fields. *Chem. Rev.* **2014**, *114*, 5057–5115. [CrossRef]
- 22. Kong, J.; Ismail, S.S.; Lu, X. Integration of inorganic nanostructures with polydopamine-derived carbon: Tunable morphologies and versatile applications. *Nanoscale* **2016**, *8*, 1770–1788. [CrossRef]
- 23. Ryu, J.H.; Messersmith, P.B.; Lee, H. Polydopamine surface chemistry: A decade of discovery. *ACS Appl. Mater. Interfaces* **2018**, *10*, 7523–7540. [CrossRef] [PubMed]
- 24. Lynge, M.E.; Van Der Westen, R.; Postma, A.; Städler, B. Polydopamine-A nature-inspired polymer coating for biomedical science. *Nanoscale* **2011**, *3*, 4916–4928. [CrossRef] [PubMed]
- 25. Huang, Q.; Chen, J.; Liu, M.; Huang, H.; Zhang, X.; Wei, Y. Polydopamine-Based functional materials and their applications in energy, environmental, and catalytic fields: State-of-the-art review. *Chem. Eng. J.* **2020**, *387*, 124019. [CrossRef]
- 26. Qu, K.; Wang, Y.; Vasileff, A.; Jiao, Y.; Chen, H.; Zheng, Y. Polydopamine-inspired nanomaterials for energy conversion and storage. *J. Mater. Chem. A* **2018**, *6*, 21827–21846. [CrossRef]
- 27. Martínez-Huerta, M.V.; Lázaro, M.J. Nanocatalysts for low temperature fuel cells. Energy Procedia 2017, 138, 14–19. [CrossRef]
- 28. Lim, S.H.; Li, Z.; Poh, C.K.; Lai, L.; Lin, J. Highly active non-precious metal catalyst based on Poly (Vinylpyrrolidone)-wrapped carbon nanotubes complexed with iron-cobalt metal ions for oxygen reduction reaction. *J. Power Sources* **2012**, 214, 15–20. [CrossRef]
- 29. Abrham, G.G.; Martínez-Huerta, M.V.; Sebastián, D.; Lázaro, M.J. Transformation of CoFe₂O₄ spinel structure into active and robust CoFe Alloy/N-doped carbon electrocatalyst for oxygen evolution reaction. *J. Colloid Interface Sci.* **2022**, *6*25, 70–82. [CrossRef]
- 30. Rangumagar, A.; Chhetri, B.; Parnell, C.; ParameswaranThankam, A.; Watanabe, F.; Mustafa, T.; Biris, A. Removal of nitrophenols from water using cellulose derived nitrogen doped graphitic carbon material containing titanium dioxide. *Part. Sci. Technol.* **2019**, 37, 444–452. [CrossRef]
- 31. Bacakova, L.; Pajorova, J.; Bacakova, M.; Skogberg, A.; Kallio, P.; Kolarova, K.; Svorcik, V. Versatile Application of Nanocellulose: From Industry to Skin Tissue Engineering and Wound Healing. *Nanomaterials* **2019**, *9*, 164. [CrossRef]
- 32. Rangumagar, A.; Chhetri, B.; ParameswaranThankam, A.; Watanabe, F.; Sinha, A.; Kim, J.-W.; Saini, V.; Biris, A. Nanocrystalline Cellulose-Derived Doped Carbonaceous Material for Rapid Mineralization of Nitrophenols under Visible Light. *ACS Omega* **2018**, 3,8111–8121. [CrossRef]
- 33. Lu, X.; Liu, Y.; He, Y.; Kuhn, A.; Shih, P.-C.; Sun, C.-J.; Wen, X.-D.; Shi, C.; Yang, H. Cobalt-Based Non-Precious Metal Catalysts Derived from Metal–Organic Frameworks for High-Rate Hydrogenation of Carbon Dioxide. *ACS Appl. Mater. Interfaces* **2019**, 11, 27717–27726. [CrossRef] [PubMed]
- 34. Jadhav, C.; Pisal, K.B.; Chavan, A.; Skakle, J.; Patil, S.; Patil, P.; Pagare, P. Electrochemical supercapacitive performance study of Spray Pyrolyzed Cobalt Oxide Film. *Mater. Today Proc.* **2021**, *43*, 2742–2746. [CrossRef]
- 35. Rusi, S.R.M. Electrodeposited Mn₃O₄-NiO-CO₃O₄ as a composite electrode material for electrochemical capacitor. *Electrochim. Acta* **2015**, *175*, 193–201. [CrossRef]
- 36. Alem, A.; Worku, A.; Ayele, D.; Habtu, N.; Ambaw, M.; Yemata, T. Enhancing pseudocapacitive properties of cobalt oxide hierarchical nanostructures via iron doping. *Heliyon* **2023**, *9*, e13817. [CrossRef]
- 37. Riley, P.; Joshi, P.; Penchev, H.; Narayan, J.; Narayan, R. One-Step Formation of Reduced Graphene Oxide from Insulating Polymers Induced by Laser Writing Method. *Crystals* **2021**, *11*, 1308. [CrossRef]
- 38. Lopez, G.P.; Castner, D.G.; Ratner, B.D. XPS O 1s binding energies for polymers containing hydroxyl, ether, ketone and ester groups. *Surf. Interface Anal.* **1991**, *17*, 267–272. [CrossRef]
- 39. Kruusenberg, I.; Matisen, L.; Tammeveski, K. Oxygen Electroreduction on multi-walled carbon nanotube supported metal phthalocyanines and porphyrins in acid media. *Int. J. Electrochem. Sci.* **2013**, *8*, 1057–1066. [CrossRef]
- 40. Miller, D.J.; Biesinger, M.C.; McIntyre, N.S. Interaction of CO₂ and CO at fractional atmosphere pressures with iron and iron oxide surfaces: One possible mechanism for surface contamination? *Surf. Interface Anal.* **2002**, *33*, 299–305. [CrossRef]
- 41. Beamson, G.; Briggs, D. *High Resolution XPS of Organic Polymers—The Scienta ESCA 300 Database*; John Wiley & Sons: Chichester, UK, 1992.
- 42. Nemoshkalenko, V.V.; Didyk, V.V.; Krivitskii, V.P.; Senekevich, A.I. Investigation of the atomic charges in iron, cobalt and nickel phosphides. *Zh. Neorg. Khimii* **1983**, *28*, 2182–2192.

43. Bonnelle, J.P.; Grimblot, J.; D'huysser, A. X-ray photoelectron spectroscopy studies of cobalt oxides. *J. Electron Spectrosc. Relat. Phenom.* **1975**, *7*, 151. [CrossRef]

- 44. Shi, R.; Chen, G.; Ma, W.; Zhang, D.; Qiu, G.; Liu, X. Shape-controlled synthesis, and characterization of cobalt oxides hollow spheres and octahedra. *Dalton Trans.* **2012**, *41*, 5981–5987. [CrossRef] [PubMed]
- 45. Jena, A.; Penki, T.R.; Munichandraiah, N.; Shivashankar, S.A. Flower-like porous cobalt(II) monoxide nanostructures as anode material for Li-ion batteries. *J. Electroanal. Chem.* **2016**, *761*, 21–27. [CrossRef]
- 46. Chuang, T.J.; Bridle, C.R.; Rice, D.W. Interaction of CO₂ and CO with clean and oxygen-covered iron surfaces. *Surf. Sci.* **1976**, *59*, 413–429. [CrossRef]
- 47. Yang, H.M.; Ouyang, J.; Tang, A.D. Preparation and characterization of cobalt oxide nanoparticles via a thermal decomposition process. *J. Phys. Chem. B* **2007**, *111*, 8006. [CrossRef]
- 48. Burriel, M.; Garcia, G.; Santiso, J.; Abrutis, A.; Saltyte, Z.; Figueras, A. Chemical vapor deposition of La₂NiO₄+δ thin films from nickelocene and lanthanum complexes. *Chem. Vap. Depos.* **2005**, *11*, 106. [CrossRef]
- 49. Dedryvere, R.; Laruelle, S.; Grugeon, S.; Poizot, P.; Gonbeau, D.; Tarascon, J.-M. Characterization of lithium alkyl carbonate species formed on electrochemically cycled graphite electrode in Li-ion batteries. *Chem. Mater.* **2004**, *16*, 1056–1061.
- 50. Gartia, Y.; Parnell, C.; Watanabe, F.; Szwedo, P.; Biris, A.; Peddi, N.; Alsudani, Z.; Ghosh, A. Graphene-Enhanced Oxygen Reduction by MN4 Type Cobalt(III) Catalyst. *ACS Sustain. Chem. Eng.* **2015**, *3*, 97–102. [CrossRef]
- 51. Ruan, M.; Liu, J.; Song, P.; Xu, W. Meta-analysis of commercial Pt/C measurements for oxygen reduction reactions via data mining. *Chin. J. Catal.* **2022**, *43*, 116–121. [CrossRef]
- 52. Jung, H.-Y.; Kim, J.; Park, J.-K. Effect of Nafion dispersion solvent on the interfacial properties between the membrane and the electrode of a polymer electrolyte membrane-based fuel cell. *Solid State Ionics* **2011**, *196*, 73–78. [CrossRef]
- 53. Nasini, U.B.; Gartia, Y.; Ramidi, P.; Kazi, A.; Shaikh, A.U.; Ghosh, A. Oxygen reduction reaction catalyzed by cobalt(III) complexes of macrocyclic ligands supported on multiwalled carbon nanotubes. *Chem. Phys. Lett.* **2013**, *566*, 38. [CrossRef]
- 54. Wayland, H.A.; Boury, S.N.; Albkuri, Y.; Watanabe, F.; Biris, A.S.; Parnell, C.M.; Ghosh, A. Graphene-Supported Cobalt(III) Complex of a Tetraamidomacrocyclic Ligand for Oxygen Reduction Reaction. *Catal. Lett.* **2018**, *148*, 407–417. [CrossRef]
- 55. Ghosh, A.; Ramidi, P.; Pulla, S.; Sullivan, S.Z.; Collom, S.L.; Gartia, Y.; Munshi, P.; Biris, A.S.; Noll, B.C.; Berry, B.C. Cycloaddition of CO₂ to Epoxides Using a Highly Active Co(III) Complex of Tetraamidomacrocyclic Ligand. *Catal. Lett.* **2010**, 137, 1–7. [CrossRef]
- 56. Rivas-Murias, B.; Salgueiriño, V. Thermodynamic CoO–Co₃O₄ crossover using Raman spectroscopy in magnetic octahedron-shaped nanocrystals. *J. Raman Spectrosc.* **2017**, *48*, 837–841. [CrossRef]
- 57. Cho, S.-H.; Jung, J.-W.; Kim, C.; Kim, I.-D. Rational Design of 1-D Co₃O₄ Nanofibers@Low content Graphene Composite Anode for High Performance Li-Ion Batteries. *Sci. Rep.* **2017**, *7*, 45105. [CrossRef]
- 58. Leng, X.; Wei, S.; Jiang, Z.; Lian, J.; Wang, G.; Jiang, Q. Carbon-Encapsulated Co₃O₄ Nanoparticles as Anode Materials with Super Lithium Storage Performance. *Sci. Rep.* **2015**, *5*, 16629. [CrossRef]

Disclaimer/Publisher's Note: The statements, opinions and data contained in all publications are solely those of the individual author(s) and contributor(s) and not of MDPI and/or the editor(s). MDPI and/or the editor(s) disclaim responsibility for any injury to people or property resulting from any ideas, methods, instructions or products referred to in the content.